

Synthesis, Structures, and Heterogeneous Catalytic Applications of {Co³⁺-Eu³⁺} and {Co³⁺-Tb³⁺} Heterodimetallic Coordination Polymers

Girijesh Kumar,^[a] Amit Pratap Singh,^[a] and Rajeev Gupta*^[a]

Keywords: Cobalt / Europium / Terbium / Polymers / Heterogeneous catalysis

Two {Co³⁺-Eu³⁺} and {Co³⁺-Tb³⁺} heterodimetallic coordination polymers have been synthesized by using a Co³⁺-based coordination complex as the building block. Structural studies show that the lanthanide atoms are coordinated to the cobalt complex through O_{amide} groups. This results in the generation of a one-dimensional zigzag coordination poly-

mer. These coordination polymers have been shown to catalyze the ring-opening reactions of the epoxides with anilines and alcohols under heterogeneous and solvent-free conditions. Interestingly, a perfect regioselectivity was observed in the aminolysis and alcoholysis reaction of styrene oxide.

Introduction

In recent years, the quest for materials with useful properties has led to intense studies on the development of inorganic-organic hybrid compounds, because they offer advantages that emerge from both metal and ligand components. Metal-organic frameworks and coordination polymers belong to this new class of materials with potential applications in gas storage, separation, sensing, and catalysis.^[1] An important characteristic of these materials is the single-site active species, in which every active site has an identical chemical environment due to the highly crystalline nature of the material. Such special features emulate enzymes with the inherent advantages of the heterogeneous catalysis.^[2]

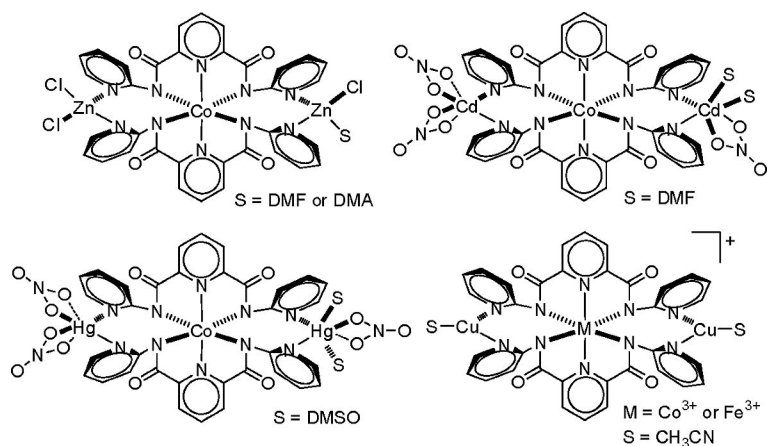
Lewis acid catalyzed organic transformation reactions are of great importance because of their unique reactivities and selectivities.^[3,4] Furthermore, such catalytic reactions often require mild reaction conditions.^[3,4] A wide variety of organic transformations by using Lewis acids have been developed, and they have been applied to the synthesis of an assorted variety of compounds. Traditionally, strong Lewis acids based on Al³⁺, B³⁺, Ti⁴⁺, and Sn⁴⁺ metal ions have been utilized;^[5] however, more than stoichiometric amounts of such Lewis acids are required in several cases. Moreover, most of these Lewis acids are moisture-sensitive and tend to decompose or deactivate in the presence of even a small amount of water.^[5] In this context, lanthanide salts, in particular, lanthanide triflates [Ln(OTf)₃], are comparatively moisture-tolerable Lewis acids and have been widely applied to a variety of organic transformations.^[6] There are,

however, several drawbacks with the routine lanthanide salts, such as recovery after the catalytic reactions and reusability. Thus, the traditional approach to Lewis acid based catalysis demands rapid change to reusable and heterogeneous catalysts. In this context, porous metal-organic frameworks and coordination polymers offer an excellent alternative to heterogeneous catalysis,^[1,2] especially those that contain lanthanide metals.^[1i]

Our group has been working on developing coordination complexes as the building blocks for the construction of ordered structures in which two different metal ions could be placed in close proximity.^[7-11] A coordination complex as the building block offer many benefits such as spectroscopic and magnetic properties as well as structural rigidity. Such an induced rigidity has the ability to place the auxiliary functional groups in a preorganized conformation with an option to control the geometrical placement of such groups. These auxiliary functional groups could then be utilized to coordinate a secondary metal ion. This synthetic strategy leads to the generation of heterodimetallic complexes^[8-10] and networks^[11] of a highly ordered nature. Utilizing this strategy, we have recently demonstrated the Co³⁺ coordination complex **1**^[7] as the building block for the preparation of {Zn²⁺-Co³⁺-Zn²⁺},^[8] {Cd²⁺-Co³⁺-Cd²⁺},^[9] and {Hg²⁺-Co³⁺-Hg²⁺}^[9] heterodimetallic complexes (Scheme 1). The selection of the peripheral metal ion was based on the possible application of the exposed Lewis-acidic metal ion in organic transformations. Indeed, the Lewis-acidic property of the peripheral metal ion was demonstrated by catalytic organic transformation reactions such as the Beckmann rearrangement of aldoximes and ketoximes, cyanation of imines, and ring-opening reactions of oxiranes and thiiranes.^[8,9,12] Interestingly, these organic transformation reactions were found to be secondary-metal-specific. Very recently, we have also synthesized {Cu⁺-M³⁺-Cu⁺} (M = Co or Fe) heterodimetallic com-

[a] Department of Chemistry, University of Delhi, Delhi 110007, India
Fax: +91-11-2766-6605
E-mail: rgupta@chemistry.du.ac.in

Supporting information for this article is available on the WWW under <http://dx.doi.org/10.1002/ejic.201000651>.



Scheme 1. Structurally characterized heterodimetallic complexes reported from our laboratory.

plexes utilizing Co^{3+} -containing building block **1** and its Fe^{3+} analogue.^[10] The peripheral Cu^I ions were shown to participate in the aerial oxidation of hindered phenols to yield carbon–carbon-coupled products as well as dealkylated products. To further understand the coordination abilities of such molecular clefts and their ability to accommodate assorted cations with variable coordination requirements, we were encouraged to look to the lanthanide metal ions. The present work explores the coordinating ability of the building block **1** towards Eu^{3+} and Tb^{3+} ions. This move was driven by the notion that the ionic radii of Eu^{3+} (1.09 Å) and Tb^{3+} (1.06 Å) are comparable to that of the Hg^{2+} ion (1.16 Å), and the structurally characterized $\{\text{Hg}^{2+}\text{-Co}^{3+}\text{-Hg}^{2+}\}$ complex has revealed that the Hg^{2+} ions can be placed within the clefts after coordination to the N_{pyridine} donors (Scheme 1). Interestingly, despite the comparable size of the Eu^{3+} and Tb^{3+} ions to that of Hg^{2+} , the lanthanide atoms opted to interact with the O_{amide} atoms rather than be placed within the clefts. This results in the generation of $\{\text{Co}^{3+}\text{-Eu}^{3+}\}$ and $\{\text{Co}^{3+}\text{-Tb}^{3+}\}$ heterodimetallic coordination polymers. Herein, we show the synthesis, structures, and catalytic applications of such coordination polymers in ring-opening reactions of epoxides with anilines and alcohols under solvent-free conditions.

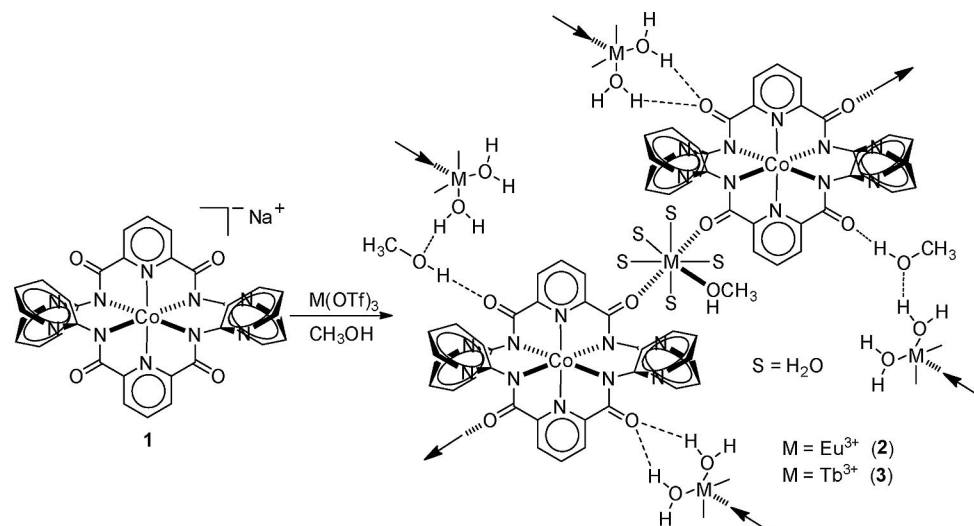
Results and Discussion

Synthesis and Characterization of **2** and **3**

The heterodimetallic complexes **2** and **3** were synthesized by treating the building block **1** with the appropriate $\text{Ln}(\text{OTf})_3$ salt in CH_3OH (Scheme 2). Both complexes were isolated as pale green crystalline materials in good yields after recrystallization from $\text{CH}_3\text{OH}/\text{Et}_2\text{O}$. They are isostructural in nature as revealed by their superimposable IR and NMR spectra and crystal structures. The FTIR spectra^[13a] of both complexes indicate the $\nu_{\text{O-H}}$ stretch at 3370–3400 cm^{-1} due to the presence of coordinated water molecules. In addition, the spectra also show the stretches for the coordinated as well as solvated CH_3OH molecules

($\nu_{\text{C-O}}$ at ca. 1175 cm^{-1}). The presence of the triflate ion was established by the observation of the $\nu_{\text{S=O}}$ stretches at around 1243–1247, 1030, and 639 cm^{-1} . The IR spectra of both **2** and **3** also show a strong band in the 1590–1595 cm^{-1} region due to the ν_{amide} stretches. A negative shift of 25–30 cm^{-1} for the ν_{amide} stretch (with respect to complex **1**) indicates the involvement of O_{amide} in the bonding. Conductivity measurements^[13b] indicate a 1:2 electrolytic nature of complexes **2** and **3** and clearly suggest that the triflate ions are not involved in coordination. The absorption spectra of complexes **2** and **3** show λ_{max} in the range of 645–650 nm that has been assigned to the d–d transition based on the Co^{3+} building block **1**^[8] (Figure S1 in the Supporting Information). Both complexes **2** and **3** were also characterized by ^1H and ^{13}C NMR spectra (Figures S2 and S3 in the Supporting Information).^[14] The NMR spectra were interpreted by comparison with that of building block **1**.^[7,8] The coordination of the Eu^{3+} and Tb^{3+} ions to **1** does not significantly alter the chemical environment of the proton or carbon atoms of the pyridyl rings. In the ^1H NMR spectra, for both complexes, the pyridyl protons were found to resonate between $\delta = 6.8$ and 8.1 ppm. For both complexes, the signal of the CH_3 group of the coordinated CH_3OH molecule was observed at $\delta \approx 3.2$ and 48.7 ppm in the ^1H and ^{13}C NMR spectra, respectively.

The thermal gravimetric analysis (TGA) for complexes **2** and **3** supports the structural analysis (cf. crystal structures). For complex **2** (Figure S4 in the Supporting Information), the observed weight loss of 14.67% fits nicely with the calculated value of 14.90% in the temperature range of 50–188 °C. This corresponds to the loss of three water molecules and a triflate ion. The second step between 330 and 540 °C corresponds to the observed weight loss of 43.94% (calcd. 43.14%), which is ascribed as the loss of one MeOH molecule, one triflate ion, and a ligand molecule. In a similar manner, complex **3** (Figure S6 in the Supporting Information) also showed a weight loss due to three water molecules and one triflate ion (found 13.21%; calcd. 14.82%) as the first step and a loss of one MeOH molecule, one triflate ion, and a ligand molecule (found 42.78%;



Scheme 2. Synthesis of coordination polymers **2** and **3**. Arrows indicate further coordination to/from the building blocks.

calcd. 42.88%) as the second step. In the differential scanning calorimetric (DSC) analysis (Figures S5 and S7 in the Supporting Information), both complexes show a combined broad feature for the loss of water molecules and triflate ions in the exothermic region of 60–165 °C. Both complexes display thermal stability up to approximately 350 °C with the observation of crystallization temperature at 352 and 358 °C for **2** and **3**, respectively.

Crystal Structures

Both heterodimetallic complexes **2** and **3** were crystallographically characterized and found to be isostructural. The molecular structures of complexes **2** and **3** are shown in Figures 1, 2, 3, and 4, whereas selected bonding parameters are contained in Tables 1 and 2. The unit cell in both cases consists of one building block (Co^{3+} complex), one lanthanide metal ion (coordinated with one methanol and five water molecules), two triflate ions, and three molecules of methanol as the solvent of crystallization. Two deprotonated tridentate ligands are arranged in a meridional fashion around the central Co^{3+} metal ion. The central Co^{3+} metal ion is coordinated by four deprotonated N_{amide} atoms in the equatorial basal plane, whereas two $\text{N}_{\text{pyridine}}$ atoms occupy the axial positions. The geometry around the Co^{3+} ion can best be described as compressed octahedral as also noted for the precursor complex **1**^[8] and other structurally characterized complexes with closely similar ligands.^[15] The average $\text{Co}\cdots\text{N}_{\text{amide}}$ and $\text{Co}\cdots\text{N}_{\text{pyridine}}$ bond lengths are 1.952 and 1.854 Å, and 1.955 and 1.862 Å for **2** and **3**, respectively. These distances are a little shorter than those of building block **1**.^[8] Moreover, the crystal structures of the heterodimetallic complexes **2** and **3** revealed that the geometry around the central Co^{3+} ion is unaffected by the coordination to the secondary metal ions. The lanthanide metal ions (Eu^{3+} for **2** and Tb^{3+} for **3**) are coordinated through the amide oxygen atoms O1 and O3 diagonally from two building blocks. This arrangement has resulted in the formation of a one-dimensional zigzag chain (Figures 3

and 4). In both complexes, Eu^{3+} and Tb^{3+} ions have eight-coordinate geometry in which five coordinations come from the water molecules and one comes from the coordinated CH_3OH molecule, whereas the remaining two sites are occupied by the O_{amide} atoms (O1 and O3) from the building blocks. The $\text{Eu}\cdots\text{O1}_{\text{amide}}$ and $\text{Eu}\cdots\text{O3}_{\text{amide}}$ bond lengths are 2.340 and 2.305 Å, respectively, whereas the $\text{Tb}\cdots\text{O1}_{\text{amide}}$ and $\text{Tb}\cdots\text{O3}_{\text{amide}}$ bond lengths were found to be 2.291 and 2.320 Å, respectively. Both O_{amide} atoms make an angle of around 146° with the lanthanide metal ion. The $\text{Eu}\cdots\text{O}_{\text{MeOH}}$ and $\text{Tb}\cdots\text{O}_{\text{MeOH}}$ distances are 2.470 and 2.445 Å for complexes **2** and **3**, respectively. The $\text{Eu}\cdots\text{O}_{\text{water}}$ and $\text{Tb}\cdots\text{O}_{\text{water}}$ bond lengths fall in the range of 2.366–2.466 Å. Interestingly, out of four O_{amide} atoms (O1, O2, O3, and O4) only two O_{amide} atoms, O1 and O3, were found to coordinate the lanthanide metal ion. Initially, this observation was puzzling; however, a closer look at the crystal structure revealed that the remaining O_{amide} atoms (O2 and

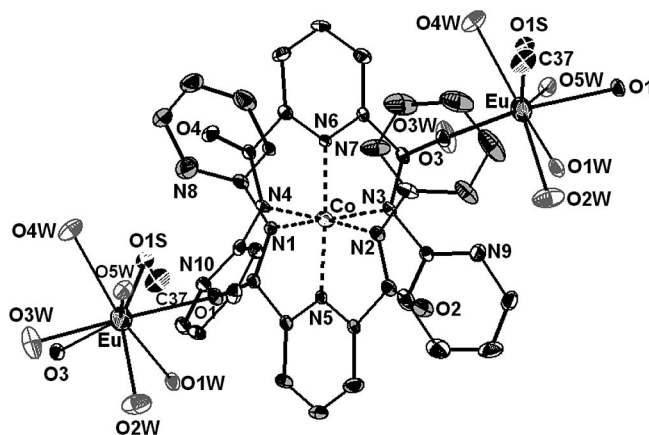


Figure 1. Partial crystal structure of **2** showing the coordination environment around the Eu^{3+} center and its bonding with the building block molecule. Thermal ellipsoids are drawn at 50% probability level; hydrogen atoms, anions, and solvent molecules have been omitted for clarity.

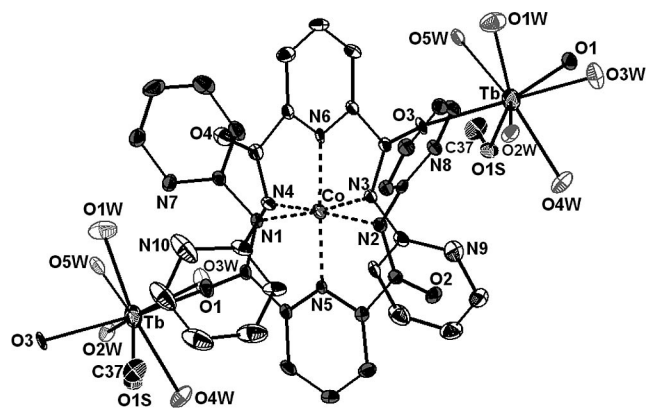


Figure 2. Partial crystal structure of **3** showing the coordination environment around the Tb^{3+} center and its bonding with the building block molecule. Thermal ellipsoids are drawn at 50% probability level; hydrogen atoms, anions, and solvent molecules have been omitted for clarity.

O4) are involved in intermolecular hydrogen bonding with the water molecules (O4W and O5W) coordinated to the lanthanide ion from the adjacent chain. Thus, two O_{amide}

Table 1. Comparative bond lengths [\AA] and bond angles [$^\circ$] around the central Co^{3+} ion for complexes **1**, **2**, and **3**.

Bond	Complex 1 ^[a]	Complex 2	Complex 3
Co–N1	1.998(7)	1.959(4)	1.961(3)
Co–N2	1.962(8)	1.955(4)	1.937(3)
Co–N3	2.048(7)	1.959(4)	1.966(3)
Co–N4	1.935(8)	1.936(4)	1.956(4)
Co–N5	1.872(7)	1.853(4)	1.863(3)
Co–N6	1.870(7)	1.856(4)	1.859(3)
N1–Co–N2	162.8(3)	163.15(15)	163.44(14)
N3–Co–N4	162.4(3)	163.43(15)	163.31(14)
N2–Co–N4	91.5(3)	92.67(15)	92.81(15)
N1–Co–N3	92.3(3)	94.23(15)	94.24(15)
N5–Co–N6	175.2(3)	176.84(16)	176.85(15)

[a] See ref.^[8]

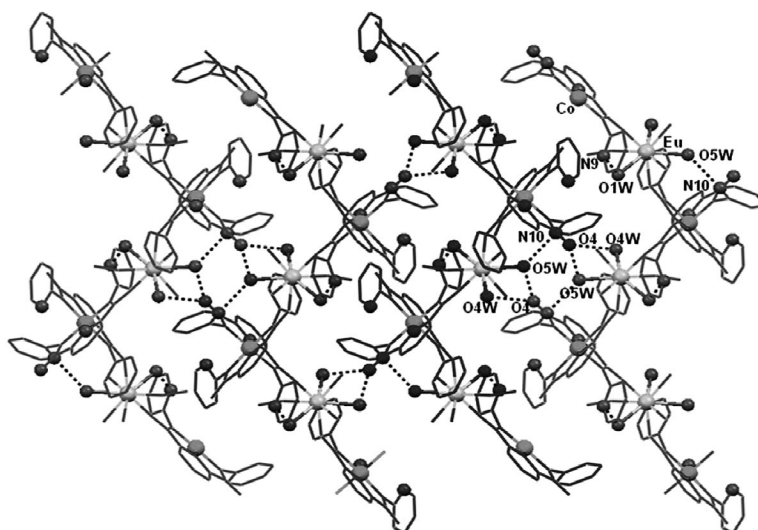


Figure 3. Weak interactions and packing diagram of coordination polymer **2**. Hydrogen atoms, anions, and solvent molecules have been omitted for clarity. See text for details.

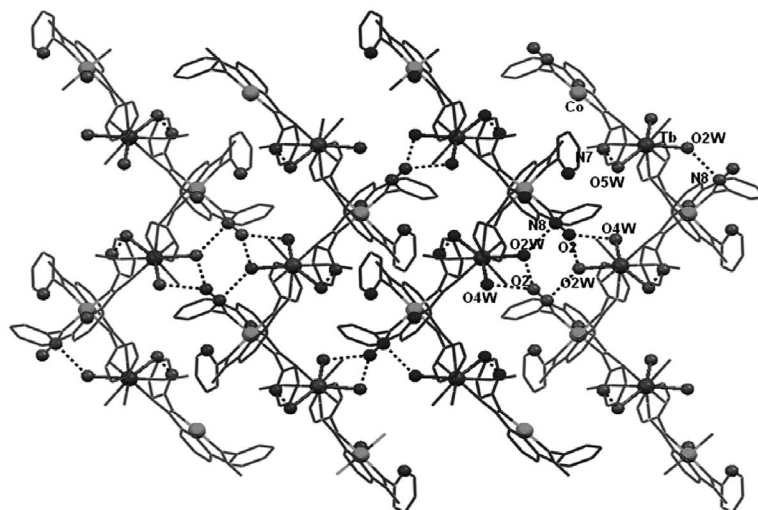


Figure 4. Weak interactions and packing diagram of coordination polymer **3**. Hydrogen atoms, anions, and solvent molecules have been omitted for clarity. See text for details.

atoms are coordinated to the lanthanide atom to generate a zigzag chain, and the remaining two O_{amide} atoms are stabilizing the secondary structure (see below).

Table 2. Comparative bond lengths [Å] and bond angles [°] around the lanthanide metal ion for complexes **2** and **3**.

Bond ^[a]	Complex 2	Complex 3
M–O1	2.340(3)	2.291(3)
M–O3	2.305(3)	2.320(3)
M–O1S	2.470(3)	2.445(4)
M–O1W	2.385(3)	2.371(4)
M–O2W	2.395(4)	2.423(3)
M–O3W	2.466(4)	2.452(4)
M–O4W	2.403(4)	2.377(3)
M–O5W	2.450(3)	2.366(3)
O1–M–O3	145.89(11)	145.68(11)
O1–M–O1W	76.14(11)	99.96(14)
O1–M–O2W	86.32(15)	140.02(12)
O1–M–O3W	140.67(12)	72.33(13)
O1–M–O4W	105.86(13)	89.67(12)
O1–M–O5W	74.38(11)	73.81(12)
O1–M–O1S	79.08(11)	77.91(12)
O3–M–O1S	78.15(11)	78.93(12)
O3–M–O1W	73.87(12)	86.46(13)
O3–M–O2W	99.83(14)	74.23(11)
O3–M–O3W	71.92(12)	140.45(12)
O3–M–O4W	89.62(12)	105.67(12)
O3–M–O5W	139.66(11)	76.20(11)
O1W–M–O1S	75.80(12)	147.50(12)
O2W–M–O1S	147.67(13)	127.64(12)
O3W–M–O1S	134.45(13)	135.02(14)
O4W–M–O1S	69.81(12)	69.95(12)
O5W–M–O1S	127.53(11)	75.81(12)

[a] M = Eu for **2** and Tb for **3**.

Weak Interactions

Both complexes **2** and **3** show various kinds of weak interactions that result in a two-dimensional (2D) network (Figures 3 and 4). In complex **2**, one zigzag strand is connected to the adjacent zigzag strand through hydrogen bonding between the amide oxygen atom O4 and water molecules O4W and O5W coordinated to the europium center. The O \cdots O heteroatom separations were found to be 2.690 and 2.683 Å, respectively. Similarly, the amide oxygen atom O4 of the second strand (symmetry-related) also forms reciprocal hydrogen bonds with the water molecules O4W and O5W of the first strand (Figure 3). The other amide atom O2 forms a hydrogen bond with the O2S atom (O2_{amide} \cdots O2S_{methanol}: 2.678 Å) of the methanol present as the solvent of crystallization. The atom O2S further interacts with O1W_{water} (O2S_{methanol} \cdots O1W: 2.679 Å) coordinated to the Eu³⁺ center. Additional intramolecular hydrogen bonds form within the strand between the hanging pyridine nitrogen atoms and the water molecules coordinated to the europium ion. For example, N_{9pyridine} forms a strong hydrogen bond with O1W_{water} with a heteroatom distance of 2.827 Å. Similarly, N_{10pyridine} forms an equally strong hydrogen bond with O5W_{water} with an N \cdots O separation of 2.797 Å. The pyridine nitrogen atom N8 forms weak hydrogen bonds, with the hydrogen atoms attached to the O4W and O5W water molecules (N \cdots O separation: ca. 3.395 Å). On the other hand, the fourth pyridine nitrogen atom N7

interacts weakly with the C–H bonds of an adjacent pyridine ring. It is important to mention that such N_{pyridine} \cdots H–O_{water} and N_{pyridine} \cdots H–C_{pyridine} hydrogen bonds lock the uncoordinated pyridine rings, thus not allowing them to interact/coordinate to the lanthanide metal ion.

A similar type of packing behavior was observed in case of the {Co³⁺–Tb³⁺} complex **3**. Two zigzag strands are connected through hydrogen bonds between the amide oxygen atom O2 and water molecules O2W and O4W with O \cdots O distances of 2.691 and 2.702 Å, respectively (Figure 4). The other amide atom O4 interacts with the O4S atom of the methanol present as the solvent of crystallization by means of a hydrogen bond (O4_{amide} \cdots O4S_{methanol}: 2.678 Å). The atom O4S further interacts with O5W_{water} (O4S_{methanol} \cdots O5W: 2.690 Å) coordinated to the Tb³⁺ center. Within a zigzag strand, hanging pyridine nitrogen atom N7 forms an intramolecular hydrogen bond with the water molecule O5W_{water} (N \cdots O separation: 2.813 Å), whereas N8 is connected to the O2W (N \cdots O separation: 2.798 Å). The pyridine atom N9 interacts much more weakly with hydrogen atoms of the water molecules O2W and O4W, with an N \cdots O separation of around 3.391 Å. As noted for complex **2**, such interactions lock the pyridine rings in this case as well.

Based on our earlier heterodimetallic complexes (Scheme 1),^[8–10] we postulated that the Eu³⁺ and Tb³⁺ ions may also be accommodated within the molecular clefts created by the hanging pyridine rings. However, the structural observation of the coordination of the Eu³⁺ and Tb³⁺ ions to O_{amide} instead of N_{pyridine} suggests the preference of lanthanide metal ions to coordinate hard donors such as O_{amide} instead of soft N_{pyridine} donors. It may be noted that the building block **1** was able to accommodate three-coordinate Cu⁺ ion (0.72 Å), four-coordinate Zn²⁺ (0.74 Å), six-coordinate Cd²⁺ (1.09 Å), and six-coordinate Hg²⁺ (1.16 Å) ions within the clefts created by the hanging pyridine rings as evidenced by the structural characterization.^[8–10] We believe there are two reasons for such an observation. First, the hard/soft acid–base concept^[16] that usurped the size factor,^[17] because the ionic radii of Eu³⁺ (1.09 Å) and Tb³⁺ (1.06 Å) are comparable to that of the Hg²⁺ ion (1.16 Å). Second, the pyridine nitrogen atoms are locked due to the formation of strong N_{pyridine} \cdots H–O_{water} hydrogen bonds and thus are not available to coordinate/accommodate the lanthanide ion.

X-ray powder diffraction (XRPD) was used to check the crystalline homogeneity and purity of the bulk product. The measured XRPD pattern closely matches the one simulated from the single-crystal diffraction data for both coordination polymers **2** and **3** (Figures S8 and S9 in the Supporting Information), thereby indicating that a single phase has resulted during the bulk synthesis of the polymers.

Solvent-Free Catalytic Applications of Networks **2** and **3**

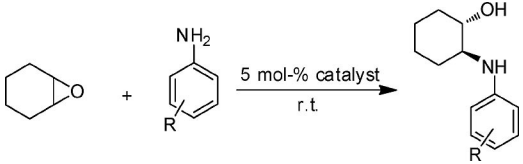
Ring-opening reactions of epoxides with various nucleophiles are attractive due to applications in the synthesis of

pharmaceutically and industrially important compounds.^[18] A variety of nucleophiles have been employed for such reactions successfully, with the majority of nucleophiles being heteroatom-based. These methodologies have provided practical access to 1,2-azido alcohols,^[19] 1,2-halohydrins,^[20] 1,2-hydroxy sulfides,^[21] 1,2-benzoyloxy alcohols,^[22] 1,2-aryloxy alcohols,^[23] 1,2-alkoxy alcohols,^[24] and 1,2-hydroxyanilines.^[25] Generally, the activation of the epoxide is a prerequisite for such reactions, and such an activation has been achieved by using a protonic acid or a metal-based Lewis acid. Several Lewis acids have been reported for the ring-opening reaction of epoxides such as metal amides,^[26] metal alkoxides,^[27] metal triflates,^[28] metal halides,^[29] and other metal salts.^[30] Compared to the well-studied ring-opening reactions of epoxides with amines, similar reactions that involve alcohols as the nucleophiles are less studied.^[31] The poor nucleophilic nature of alcoholic substrates has been suggested as the potential reason and led to the use of strong acidic or basic media for carrying out such reactions.^[32] Thus, there is a need for a widely applicable approach whereby a common catalyst could perform ring-opening reactions by using both amines and alcohols as the nucleophile under ambient conditions. The $\{\text{Co}^{3+}\text{-Eu}^{3+}\}$ and $\{\text{Co}^{3+}\text{-Tb}^{3+}\}$ heterodimetallic coordination polymers are shown here to act as heterogeneous catalysts for the aminolysis and alcoholysis reactions under solvent-free conditions.

For the aminolysis reaction, an equimolar mixture of cyclohexene oxide and aniline was stirred under solvent-free conditions at room temperature in the presence of catalyst (5 mol-% **2** or **3**). Under these conditions, a smooth reaction took place and, after workup, the respective product, β -amino alcohol, was isolated in high yield. As shown in the Table 3, the coordination polymers **2** and **3** could promote the reaction between the cyclohexene oxide with aniline (Entry 1) and *para*-substituted anilines that contain various functional groups (Entries 2–6). Without catalysts **2** or **3**, the reaction did not proceed at all, thereby supporting the possible Lewis-acidic metal-catalyzed activity of the coordination polymers. Further, when the catalyst was filtered off, the reaction was no longer promoted. A control experiment of using the building block **1** also did not result in any product formation. However, a reaction by using $\text{Eu}(\text{OTf})_2$ or $\text{Tb}(\text{OTf})_2$ as a catalyst^[6a] under homogeneous conditions (with THF as the solvent) did result in <20% conversion, thus demonstrating the enhanced catalytic activity of coordination polymers **2** and **3** under heterogeneous and solvent-free conditions. These experiments clearly show that the soluble and catalytically active species are not eluted at all from coordination polymers **2** and **3** under the reaction conditions. Thus, the reaction does proceed by heterogeneous catalysis of the coordination polymers. In addition, the catalysts can be recovered after the reaction and reused several times (tested six times; Table 3, Entry 1) without significant loss of activity (<5% drop in isolated yield in the sixth run). The recovered coordination polymers **2** and **3** were characterized by XRPD and FTIR spectra before and after the catalytic reaction and showed

identical results. A comparison of XRPD patterns of catalysts **2** and **3** before and after the catalytic reaction did not reveal significant differences (Figures S10 and S11 in the Supporting Information) and thus strongly suggests that the structural integrity of the material is preserved after the catalytic reaction. The effect of electronic substituents on the product yield was evaluated by the placement of electron-donating and -withdrawing groups at the *para* position of the aniline ring. As anticipated, the yields were higher with electron-rich anilines (Table 3, Entries 2 and 3) due to the better nucleophilicity than with electron-poor anilines (Entries 4–6). A similar observation has been noticed in the literature.^[9,33,34] For example, in the case of *para*-nitroaniline, for both catalysts **2** and **3**, the yield dropped to less than 10% (Entry 6) even when the reaction was carried out for 24 h as compared to 4 h in other cases.

Table 3. Ring-opening reactions of cyclohexene oxide with aniline and *para*-substituted anilines by using catalysts **2** and **3**.



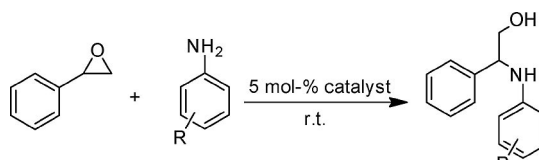
Entry	R	Time [h] ^[b]	Yield [%] ^[a]	
			Catalyst 2	Catalyst 3
1	H	4	98, 96, ^[b] 94 ^[c]	98, 95, ^[b] 94 ^[c]
2	C ₂ H ₅	4	90	99
3	CH ₃ O	4	72	66
4	Cl	4	63	58
5	F	4	46	32
6	NO ₂	24	8	6

[a] Isolated yield. [b] Third run with reused catalyst. [c] Sixth run with reused catalyst.

To determine the regioselectivity, styrene oxide was used as a representative unsymmetrical epoxide^[33,34] and was treated with aniline or *para*-substituted anilines in the presence of catalyst **2** or **3** (5 mol-%; Table 4). Interestingly, a perfect regioselectivity was observed that resulted in only a single product in all cases with both catalysts **2** and **3**. Out of two possible products due to the nucleophilic attack either at the benzylic carbon atom or at the less hindered carbon atom of the epoxide ring, in all cases, nucleophilic attack took place at the benzylic carbon atom of the epoxide. The regioisomer formed by the reaction of the amine at the benzylic carbon atom of the epoxide ring showed the characteristic molecular ion peak $[\text{M}^+ - 31]$ due to the loss of the CH_2OH fragment in the GC–MS studies.^[33] This conclusively proves a single product, as the other regioisomer is expected to show the molecular ion peak $[\text{M}^+ - 107]$ due to the loss of the $\text{C}_6\text{H}_5\text{CHOH}$ fragment for the product formed by the reaction at the terminal carbon atom of the epoxide ring.^[33] These results indicate that the epoxide ring has interacted with the lanthanide ion through the less-hindered side, possibly due to steric reasons caused by the attached pyridine rings and solvent molecules. As noted for the cyclohexene oxide, here also the yields were found

to be higher with electron-rich anilines (Table 4, Entries 2 and 3) than with electron-poor ones (Entries 4–6). In addition, the reused catalysts were able to catalyze the reaction efficiently several times without any further purification or regeneration (tested six times; Table 4, Entry 1).

Table 4. Ring-opening reactions of styrene oxide with aniline and *para*-substituted anilines by using catalysts **2** and **3**.



Entry	R	Time [h] ^[b]	Yield [%] ^[a]	
			Catalyst 2	Catalyst 3
1	H	4	83, 80, ^[b] 76 ^[c]	98, 96, ^[b] 94 ^[c]
2	C ₂ H ₅	4	85	99
3	CH ₃ O	4	65	68
4	Cl	4	55	52
5	F	4	12	85
6	NO ₂	24	4	7

[a] Isolated yield. [b] Third run with reused catalyst. [c] Sixth run with reused catalyst.

The heterogeneous catalytic reactions were then extended to alcoholysis by using alcohols as the nucleophile.^[31,32,35] Both cyclohexene oxide and styrene oxide were opened with few alcoholic substrates carrying various steric groups (isopropyl alcohol, *sec*-butyl alcohol, *tert*-butyl alcohol, and benzyl alcohol) in the presence of catalyst **2** or **3** (5 mol-%). In general, the alcoholysis reactions were found to take longer (24 h), and the results indicate poorer transformations than the corresponding aminolysis reactions (Table 5). Out of several alcohols tested, *tert*-butyl alcohol was found to be the best (Table 5, Entries 1 and 5), whereas benzyl alcohol poorly promoted the ring-opening reaction (Entries 4 and 8). This could be explained by the electron-donating character of the *tert*-butyl group in the former and the electron-withdrawing effect of the benzene ring in the latter. In the case of cyclohexene oxide, products were obtained as the single diastereoisomer with *trans* stereochem-

istry.^[35] The styrene oxide always led to the formation of one regioisomer, through incorporation of the alcohol at the phenyl-substituted carbon atom, irrespective of the nature of the alcohol, as expected for a charge-controlled ring-opening process.^[36] A similar observation was made for the aminolysis reactions that used styrene oxide as an unsymmetrical epoxide. All control experiments showed no conversion, even after prolonged reaction time (up to 72 h).

Conclusion

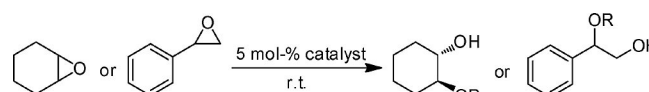
Two new {Co³⁺–Eu³⁺} and {Co³⁺–Tb³⁺} coordination polymers **2** and **3**, respectively, have been synthesized and characterized. The crystallographic investigations show that the lanthanide ions are connected to the building-block cobalt complex through O_{amide} groups. This results in the generation of a one-dimensional zigzag coordination polymer. Furthermore, the individual chains were found to connect to each other through several hydrogen bonds that result in the generation of a two-dimensional network. These coordination polymers have been shown to catalyze the ring-opening reactions of epoxides with anilines and alcohols under heterogeneous and solvent-free conditions. Interestingly, a perfect regioselectivity was observed in the aminolysis and alcoholysis ring-opening reaction of styrene oxide. Future studies will target harnessing the presence of both the Lewis acidity of the lanthanide ion and the Brønsted basicity of the uncoordinated pyridine rings in a multifunctional catalytic endeavor.

Experimental Section

Materials and Reagents: The solvents were purified as reported before.^[37–41] The ligand H₂L¹ and complex Na[Co(L¹)₂] (**1**) were synthesized according to our earlier reports.^[7,8]

Synthesis of [{Co(L¹)₂–Eu(OH)₂}(CH₃OH)](CF₃SO₃)₂·3CH₃OH]_n (2**):** Complex **2** was synthesized by treating a solution of Eu(CF₃SO₃)₃ (669 mg, 1.116 mmol) in CH₃OH (2 mL) with a solution of complex **1** (400 mg, 0.558 mmol) in CH₃OH (4 mL). The reaction mixture was stirred at room temperature for 2 h. The solu-

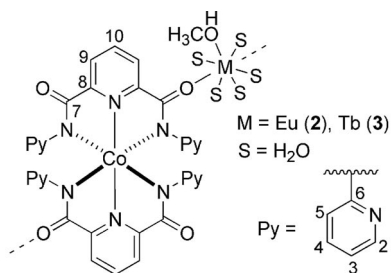
Table 5. Ring-opening reactions of cyclohexene oxide and styrene oxide with alcohols by using catalysts **2** and **3**.^[a]



Entry	Epoxide ^[b]	Alcohol	Product R–	Yield [%] ^[c]	
				Catalyst 2	Catalyst 3
1	C.O.	(CH ₃) ₃ COH	(CH ₃) ₃ C–	65	58
2	C.O.	CH ₃ CH ₂ CH(CH ₃)OH	CH ₃ CH ₂ CH(CH ₃)–	60	55
3	C.O.	(CH ₃) ₂ CHOH	(CH ₃) ₂ CH–	55	50
4	C.O.	C ₆ H ₅ CH ₂ OH	C ₆ H ₅ CH ₂ –	30	24
5	S.O.	(CH ₃) ₃ COH	(CH ₃) ₃ C–	74	54
6	S.O.	CH ₃ CH ₂ CH(CH ₃)OH	CH ₃ CH ₂ CH(CH ₃)–	56	55
7	S.O.	(CH ₃) ₂ CHOH	(CH ₃) ₂ CH–	56	55
8	S.O.	C ₆ H ₅ CH ₂ OH	C ₆ H ₅ CH ₂ –	25	24

[a] Reaction time: 24 h. [b] C.O. and S.O. stand for cyclohexene oxide and styrene oxide, respectively. [c] Isolated yield.

tion was filtered through a pad of Celite in a medium-porosity frit, and the solvent was evaporated under reduced pressure. The crude product thus obtained was redissolved in methanol and vapors of diethyl ether were diffused at room temperature. After a period of 3–4 d, pale green crystalline material was obtained that was filtered and dried under vacuum. Yield: 360 mg (65%). $C_{40}H_{48}CoEuF_6N_{10}O_{19}S_2$ (1361.88): calcd. C 33.00, H 3.19, N 10.45; found C 33.84, H 3.34, N 10.89. FTIR (KBr, selected peaks): $\tilde{\nu}$ = 3400 (OH), 1593, 1556 (C=O), 1247, 1030, 639 (S–O), 1175 (O–CH₃) cm^{-1} . Conductivity (ca. 1 mM solution, 298 K): Λ_M = 130 (in CH₃OH), 115 (in DMF), 175 (in CH₃CN), 60 (in DMSO) $\Omega^{-1}cm^2mol^{-1}$. Absorption (DMSO): λ_{max} (ϵ) = 645 (165), 470 (sh, 210 $M^{-1}cm^{-1}$) nm. FAB-MS: calcd. for $\{[Co(L^1)_2-Eu(CH_3OH)_4(H_2O)_5(OTf)_2] + K^+\}$ 1396.98; found 1397. ¹H NMR ($[D_6]DMSO$, 300 MHz, 25 °C, TMS): δ = 8.04 (t, J = 7.2 Hz, 2 H, 10-H), 7.67 (4 H, 2-H), 7.58 (d, J = 9 Hz, 4 H, 5-H), 7.28 (m, 4 H, 4-H), 7.03 (br. d, J = 6 Hz, 4 H, 9-H), 6.70, (br. m, 4 H, 3-H), 3.2 (s, 3 H, CH₃ of CH₃OH) ppm. ¹³C NMR ($[D_6]DMSO$, 300 MHz, 25 °C, TMS): δ = 147.37 (C-2), 122.30 (C-3), 122.95 (C-4), 117.97 (C-5), 157.25 (C-6), 167.25 (C-7), 159.76 (C-8), 135.46 (C-9), 138.66 (C-10), 48.72 (CH₃ of CH₃OH) ppm.



Synthesis of $\{[Co(L^1)_2-Tb(OH_2)_5(CH_3OH)](CF_3SO_3)_2 \cdot 3CH_3OH\}_n$ (3): This compound was synthesized in a similar manner as complex **2** by using $Tb(CF_3SO_3)_3$. Yield: 400 mg (62%). $C_{40}H_{48}CoF_6N_{10}O_{19}S_2Tb$ (1368.84): calcd. C 32.55, H 3.18, N 10.72; found C 32.05, H 3.15, N 10.34. FTIR (KBr, selected peaks): $\tilde{\nu}$ = 3370 (OH), 1594, 1558 (C=O), 1243, 1030, 639 (S–O), 1174 (O–CH₃) cm^{-1} . Conductivity (ca. 1 mM solution, 298 K): Λ_M = 135 (in CH₃OH), 145 (in DMF), 165 (in CH₃CN), 62 (in DMSO) $\Omega^{-1}cm^2mol^{-1}$. Absorption (DMSO): λ_{max} (ϵ) = 646 (170), 472 (sh, 205 $M^{-1}cm^{-1}$) nm. FAB-MS: calcd. for $\{[Co(L^1)_2-Tb(CH_3OH)_4(H_2O)_5(OTf)_2]+K^+\}$ 1403.94; found 1404. ¹H NMR ($[D_6]DMSO$, 300 MHz, 25 °C, TMS): δ = 7.86 (br., 2 H, 10-H), 7.65 (br., 4 H, 2-H), 7.44 (br., 4 H, 5-H), 7.22 (br., 4 H, 4-H), 6.98 (br., 4 H, 9-H), 6.64, (br., 4 H, 3-H), 3.2 (s, 3 H, CH₃ of CH₃OH) ppm. ¹³C NMR ($[D_6]DMSO$, 300 MHz, 25 °C, TMS): δ = 147.31 (C-2), 122.19 (C-3), 122.87 (C-4), 117.85 (C-5), 157.31 (C-6), 167.06 (C-7), 159.76 (C-8), 135.32 (C-9), 138.50 (C-10) ppm.

Physical Measurements: The conductivity measurements were carried out in organic solvents with a digital conductivity bridge from the Popular Traders, India (model number: PT 825). The elemental analysis data were obtained with an Elementar Analysen Systeme GmbH Vario EL-III instrument. The NMR spectroscopic measurements were carried out with a Bruker Avance (300 MHz) instrument. The IR spectra (either as KBr pellet or as a mull in mineral oil) were recorded with a Perkin–Elmer FTIR 2000 spectrometer. The absorption spectra were recorded with a Perkin–Elmer Lambda 25 spectrophotometer. GC–MS studies were performed with a Shimadzu instrument (QP 2010) with an RTX-5SIL-MS column. The FAB mass spectra were recorded with a Jeol SX 102/Da-600 instrument. Thermal gravimetric analysis (TGA) and differential scanning calorimetry (DSC) were performed with DTG 60 Shi-

madzu and TA-DSC Q200 instruments, respectively, at 5 °C min^{-1} heating rate under nitrogen. The X-ray powder diffraction studies were performed either with an X'Pert Pro from Panalytical or a Bruker AXS D8 Discover instrument (Cu- K_α radiation, λ = 1.54184 Å). The samples were ground and subjected to the range of θ = 2–50° with a scan rate of 1° per minute at room temperature.

Crystallography: Single crystals suitable for the X-ray diffraction studies were grown by vapor diffusion of diethyl ether to a solution of the complex in CH₃OH in both cases. The intensity data for complexes **2** and **3** were obtained with a Bruker Kappa Apex-CCD diffractometer by using graphite-monochromated Mo- K_α radiation (λ = 0.71073 Å) at 293K.^[42,43] Intensity data were corrected for Lorentz polarization effects, and an empirical absorption correction (SADABS) was applied.^[44] The structures were solved by direct methods and refined by full-matrix least-squares refinement techniques on F^2 by using the programs SHELXL-97 in the WinGX module.^[45] All hydrogen atoms were fixed at calculated positions with isotropic thermal parameters, whereas all non-hydrogen atoms were refined anisotropically. Details of the crystallographic data collection and structural solution parameter are given in Table 6. CCDC-780429 (**2**) and -780430 (**3**) contain the supplementary crystallographic data for this paper. These data can be obtained free of charge from The Cambridge Data Center via www.ccdc.cam.ac.uk/data_request/cif.

Table 6. Crystallographic data collection and structural refinement parameters for complexes **2** and **3**.

	2	3
Empirical formula	$C_{40}H_{48}CoEuF_6N_{10}O_{19}S_2$	$C_{40}H_{48}CoF_6N_{10}O_{19}S_2Tb$
Formula mass	1361.89	1368.85
T [K]	293(2)	293(2)
Crystal system	monoclinic	monoclinic
Space group	$P2_1/n$	$P2_1/n$
a [Å]	15.225(5)	15.235(5)
b [Å]	18.546(5)	18.531(5)
c [Å]	19.479(5)	19.469(5)
α [°]	90	90
β [°]	105.944(5)	105.849(5)
γ [°]	90	90
V [Å ³]	5289(3)	5288(3)
Z	4	4
d [g cm^{-3}]	1.710	1.720
μ [mm ⁻¹]	1.670	1.822
$F(000)$	2744	2752
R (int.)	0.0576	0.0565
Final R indices	$R1 = 0.0429$	$R1 = 0.0455$
$[I > 2\sigma(I)]^{[a]}$	$wR2 = 0.1188$	$wR2 = 0.1277$
R indices (all data)	$R1 = 0.0694$	$R1 = 0.0590$
$wR2$ (all data)	$wR2 = 0.1475$	$wR2 = 0.1522$
GOF on F^2	1.112	1.091

$$[a] R_1 = \Sigma ||F_o| - |F_c|| / \Sigma |F_o|; wR = \{ \Sigma [w(F_o^2 - F_c^2)^2] / \Sigma wF_o^4 \}^{1/2}.$$

General Procedure for the Catalytic Reactions: The ring-opening reactions of the epoxides were carried out in oven-dried glassware under an inert gas. In a typical aminolysis reaction, cyclohexene oxide (0.98 mmol) was treated with aniline (1.18 mmol) in the presence of catalyst **2** or **3** (0.0495 mmol). However, in case of styrene oxide, the epoxide (0.875 mmol) was treated with aniline (1.05 mmol) in the presence of catalyst **2** or **3** (0.0438 mmol). For the alcoholysis reactions, epoxide (0.98 mmol) and catalyst **2** or **3** (0.0495 mmol) were stirred in alcohol (2 mL) at room temperature for 24 h. The reactions were monitored by thin-layer chromatography (TLC). After 4 h, the catalyst was filtered off, and the filtrate was concentrated under reduced pressure. The crude product was

purified by flash column chromatography on silica gel using a hexane/ethyl acetate mixture (5:1) as the eluent. The products were isolated and analyzed by GC/GC–MS techniques. The recovered catalyst was washed with diethyl ether, dried, and reused without further purification or regeneration. Moreover, the recovered catalysts were characterized by X-ray powder diffraction and FTIR spectra and showed identical results to those of the fresh samples.

Supporting Information (see footnote on the first page of this article): Figures for the absorption spectra (Figure S1), NMR spectra (Figures S2 and S3), thermal gravimetric analysis (Figures S4 and S6), differential scanning calorimetry (Figures S5 and S7), and X-ray powder diffraction (Figures S8–S11).

Acknowledgments

R. G. gratefully acknowledges the generous financial support of the Department of Science and Technology (DST), New Delhi. Crystallographic data collection was provided by IIT-Roorkee (Professor U. P. Singh). The AIRF center of JNU, New Delhi served as the GC–MS and XRPD facility. FAB-MS spectra were provided by SAIF-CDRI, Lucknow. A. P. S thanks the Council of Scientific and Industrial Research (CSIR) for the award of an SRF fellowship.

- [1] a) M. Eddaoudi, D. B. Moler, H. Li, B. Chen, T. M. Reineke, M. O’Keeffe, O. M. Yaghi, *Acc. Chem. Res.* **2001**, *34*, 319; b) M. Fujita, M. Tominaga, A. Hori, B. Therrien, *Acc. Chem. Res.* **2005**, *38*, 369; c) J. L. C. Rowsell, O. M. Yaghi, *Angew. Chem. Int. Ed.* **2005**, *44*, 4670; d) J. T. Hupp, K. R. Poeppelmeier, *Science* **2005**, *309*, 2008; e) A. G. Wong-Foy, A. J. Matzger, O. M. Yaghi, *J. Am. Chem. Soc.* **2006**, *128*, 3494; f) H. Wu, W. Zhou, T. Yildirim, *J. Am. Chem. Soc.* **2007**, *129*, 5314; g) M. Yoshizawa, J. K. Klosterman, M. Fujita, *Angew. Chem.* **2009**, *48*, 3418; h) D. J. Tranchemontagne, J. L. Mendoza-Cortes, M. O’Keeffe, O. M. Yaghi, *Chem. Soc. Rev.* **2009**, *38*, 1257; i) T. M. Reineke, M. Eddaoudi, M. O’Keeffe, O. M. Yaghi, *Angew. Chem. Int. Ed.* **1999**, *38*, 2590.
- [2] U. Muller, M. M. Schubert, O. M. Yaghi, in *Handbook of Heterogeneous Catalysis* (Eds.: G. Ertl, H. Knozinger, F. Schuth, J. Weitkamp), Wiley-VCH, Weinheim, **2008**, p. 247.
- [3] a) D. Schinzer, *Selectivities in Lewis Acid Promoted Reactions*, Kluwer Academic Publishers, Dordrecht, **1989**; b) *Lewis Acids in Organic Synthesis* (Ed.: H. Yamamoto), Wiley-VCH, Weinheim, **2000**.
- [4] a) R. D. Howells, J. C. McCown, *Chem. Rev.* **1977**, *77*, 69; b) H. Emde, D. Domsch, H. Feger, U. Frick, A. Goyz, H. H. Hergett, K. Hofmann, W. Kober, K. Krageloh, T. Oesterle, W. Steppan, W. West, G. Simchen, *Synthesis* **1982**, *1*; c) P. J. Stang, M. Hanack, L. R. Subramanian, *Synthesis* **1982**, 85; d) P. J. Stang, M. R. White, *Aldrichim. Acta* **1983**, *16*, 15.
- [5] a) T. Inoue, T. Mukaiyama, *Bull. Chem. Soc. Jpn.* **1980**, *53*, 174; b) S. Murata, M. Suzuki, R. Noyori, *J. Am. Chem. Soc.* **1980**, *102*, 3248; c) T. Mukaiyama, N. Iwasawa, R. W. Stevens, T. Haga, *Tetrahedron* **1984**, *40*, 1381; d) T. Sato, J. Otera, H. Nozaki, *J. Am. Chem. Soc.* **1990**, *112*, 901; e) N. Minowa, T. Mukaiyama, *Chem. Lett.* **1987**, 1719; f) G. A. Olah, O. Farooq, S. Morteza, F. Farnia, J. A. Olah, *J. Am. Chem. Soc.* **1988**, *110*, 2560; g) E. J. Corey, K. Shimoji, *J. Am. Chem. Soc.* **1983**, *105*, 1662.
- [6] a) S. Kobayashi, M. Sugiura, H. Kitagawa, W. W.-L. Lam, *Chem. Rev.* **2002**, *102*, 2227; b) M. Shibasaki, N. Yoshikawa, *Chem. Rev.* **2002**, *102*, 2187; c) S. Kobayashi, *Synlett* **1994**, 689; d) R. W. Marshman, *Aldrichim. Acta* **1995**, *28*, 77; e) S. Kobayashi, *Justus Liebigs Ann. Chem.* **1950**, *15*, 5; f) S. Kobayashi, *Chem. Lett.* **1991**, 2187.
- [7] A. Mishra, N. K. Kaushik, A. K. Verma, R. Gupta, *Eur. J. Med. Chem.* **2008**, *43*, 2189.
- [8] A. Mishra, A. Ali, S. Upreti, R. Gupta, *Inorg. Chem.* **2008**, *47*, 154.
- [9] A. Mishra, A. Ali, S. Upreti, M. S. Whittingham, R. Gupta, *Inorg. Chem.* **2009**, *48*, 5234.
- [10] A. P. Singh, R. Gupta, *Eur. J. Inorg. Chem.* **2010**, 4546.
- [11] A. P. Singh, A. Ali, R. Gupta, *Dalton Trans.* **2010**, *39*, 8135.
- [12] A. Ali, A. P. Singh, R. Gupta, *J. Chem. Sci.* **2010**, *122*, 311.
- [13] a) K. Nakamoto, *Infrared and Raman Spectra of Inorganic and Coordination Compounds*, Wiley, **1986**; b) W. J. Geary, *Coord. Chem. Rev.* **1971**, *7*, 81.
- [14] It is important to mention that, although the coordination polymers **2** and **3** dissolve in [D₆]DMSO and their ¹H and ¹³C NMR spectra were recorded, the exact identity of the species present during the spectral analysis is not clear. It is likely that these coordination polymers are fragmented to their molecular components or some oligomers.
- [15] a) M. Ray, D. Ghosh, Z. Shirin, R. Mukherjee, *Inorg. Chem.* **1997**, *36*, 3568; b) A. K. Patra, R. Mukherjee, *Inorg. Chem.* **1999**, *38*, 1388; c) A. K. Singh, V. Balamurugan, R. Mukherjee, *Inorg. Chem.* **2003**, *42*, 6497; d) J. L. Bricks, G. Reck, K. Rurack, B. Schulz, M. Spieless, *Supramol. Chem.* **2003**, *15*, 189.
- [16] J.-C. Claude, G. Bunzli, *Acc. Chem. Res.* **2006**, *39*, 53.
- [17] D. Hannachi, N. Ouddai, H. Chermette, *Dalton Trans.* **2010**, 3673.
- [18] a) M. E. Connolly, F. Kersting, C. T. Dollery, *Prog. Cardiovasc. Dis.* **1976**, *19*, 203; b) D. J. Triggle, in *Burger’s Medicinal Chemistry*, 4th ed. (Ed.: M. S. Wolff), Wiley-Interscience, New York, **1981**, p. 225; c) J. De Cree, H. Geukens, J. Leempoels, H. Verhaegen, *Drug Dev. Res.* **1986**, *8*, 109; d) R. R. Young, J. H. Gowen, B. T. Shahani, *N. Engl. J. Med.* **1975**, *293*, 950; e) J. Joossens, P. Vander-Veken, A. M. Lambeir, K. Augustyns, A. Haemers, *J. Med. Chem.* **2004**, *47*, 2411; f) D. M. Hodgson, A. R. Gibbs, G. P. Lee, *Tetrahedron* **1996**, *52*, 14361; g) E. N. Jacobsen, M. H. Wu, in *Comprehensive Asymmetric Catalysis* (Eds.: E. N. Jacobsen, A. Pfaltz, H. Yamamoto), Springer, New York, **1999**, chapter 35.
- [19] a) W. A. Nugent, *J. Am. Chem. Soc.* **1992**, *114*, 2768; b) L. E. Martinez, J. L. Leighton, D. H. Carsten, E. N. Jacobsen, *J. Am. Chem. Soc.* **1995**, *117*, 5897; c) S. E. Schaus, J. F. Larrow, E. N. Jacobsen, *J. Org. Chem.* **1997**, *62*, 4197.
- [20] a) S. E. Denmark, P. A. Barsanti, K.-T. Wong, R. A. Stavenger, *J. Org. Chem.* **1998**, *63*, 2428; b) W. A. Nugent, *J. Am. Chem. Soc.* **1998**, *120*, 7139.
- [21] a) T. Iida, N. Yamamoto, H. Sasai, M. Shibasaki, *J. Am. Chem. Soc.* **1997**, *119*, 4783; b) M. H. Wu, E. N. Jacobsen, *J. Org. Chem.* **1998**, *63*, 5252.
- [22] E. N. Jacobsen, F. Kakiuchi, R. G. Konsler, J. F. Larrow, M. Tokunaga, *Tetrahedron Lett.* **1997**, *38*, 773.
- [23] T. Iida, N. Yamamoto, S. Matsunaga, H.-G. Woo, M. Shibasaki, *Angew. Chem. Int. Ed.* **1998**, *37*, 2223.
- [24] a) P. Stead, H. Marley, M. Mahmoudian, G. Webb, D. Noble, Y. T. Ip, E. Piga, T. Rossi, S. Roberts, M. J. Dawson, *Tetrahedron: Asymmetry* **1997**, *7*, 2247; b) J. Xin, J. Suo, X. Zhang, Z. Zhang, *New J. Chem.* **2000**, *24*, 569; c) C. J. Salomon, *Synlett* **2001**, 65.
- [25] a) S. Sagawa, H. Abe, Y. Hase, T. Inaba, *J. Org. Chem.* **1999**, *64*, 4962; b) A. Sekine, T. Ohshima, M. Shibasaki, *Tetrahedron* **2002**, *58*, 75; c) G. Bartoli, M. Bosco, A. Carlone, M. Locatelli, M. Massaccesi, P. Melchiorre, L. Sambri, *Org. Lett.* **2004**, *6*, 2173; d) G. Bartoli, M. Bosco, A. Carlone, M. Locatelli, P. Melchiorre, L. Sambri, *Org. Lett.* **2004**, *6*, 3973; e) C. Schneider, A. R. Sreekanth, E. Mai, *Angew. Chem. Int. Ed.* **2004**, *43*, 5691; f) F. Carree, R. Gil, J. Collin, *Org. Lett.* **2005**, *7*, 1023.
- [26] J. Yamada, M. Yumoto, Y. Yamamoto, *Tetrahedron Lett.* **1989**, *30*, 4255.
- [27] S. Sagawa, H. Abe, Y. Hase, T. Inaba, *J. Org. Chem.* **1999**, *64*, 4962.

- [28] a) J. Auge, F. Leroy, *Tetrahedron Lett.* **1996**, *37*, 7715; b) M. Chini, P. Crosti, L. Favero, M. Macchia, M. Pineschi, *Tetrahedron Lett.* **1994**, *35*, 433; c) M. Meguro, N. Asao, Y. Yamamoto, *J. Chem. Soc. Perkin Trans. 1* **1994**, 2597; d) T. Ollevier, G. Lavie-Compin, *Tetrahedron Lett.* **2004**, *45*, 49.
- [29] a) L. R. Reddy, M. A. Reddy, N. Bhanumathi, K. R. Rao, *Synthesis* **2001**, 831; b) A. K. Chakraborti, A. Kondaskar, *Tetrahedron Lett.* **2003**, *44*, 8315.
- [30] a) P. Q. Zhao, L. W. Xu, C. G. Xia, *Synlett* **2004**, 846; b) A. Kamal, R. Ramu, M. A. Azhar, G. B. R. Khanna, *Tetrahedron Lett.* **2005**, *46*, 2675.
- [31] a) J. G. Smith, *Synthesis* **1984**, 629; b) C. J. Salomon, *Synlett* **2001**, 65; c) J. Xin, J. Suo, X. Zhang, *New J. Chem.* **2000**, *24*, 569.
- [32] a) A. B. Smith III, N. J. Liverton, N. J. Hrib, H. Sivaramakrishnan, K. Winzenberg, *J. Am. Chem. Soc.* **1986**, *108*, 3040; b) Y. Izumi, K. Hayashi, *Chem. Lett.* **1980**, 787; c) T. Mall, H. Stamm, *J. Org. Chem.* **1987**, *52*, 4812.
- [33] Shivani, B. Pujala, A. K. Chakraborti, *J. Org. Chem.* **2007**, *72*, 3713.
- [34] G. Mancillia, M. Femenia-Rios, A. J. Macias-Sanchez, I. G. Collado, *Tetrahedron* **2008**, *64*, 11732.
- [35] J. Barluenga, H. Vazquez-Villa, A. Ballesteros, J. M. Gonzalez, *Org. Lett.* **2002**, *4*, 2817 and references cited therein.
- [36] E. G. Lewars, in *Comprehensive Heterocyclic Chemistry* (Eds.: A. R. Katritzky, C. W. Rees, W. Lwowski), Pergamon, Oxford, **1984**, vol. 7, p. 100.
- [37] S. K. Sharma, S. Upreti, R. Gupta, *Eur. J. Inorg. Chem.* **2007**, 3247.
- [38] J. Singh, G. Hundal, R. Gupta, *Eur. J. Inorg. Chem.* **2008**, 2052.
- [39] J. Singh, G. Hundal, R. Gupta, *Eur. J. Inorg. Chem.* **2009**, 3259.
- [40] S. K. Sharma, G. Hundal, R. Gupta, *Eur. J. Inorg. Chem.* **2010**, 621.
- [41] J. Singh, G. Hundal, M. Corbella, R. Gupta, *Polyhedron* **2007**, *26*, 3893.
- [42] *SMART: Bruker Molecular Analysis Research Tool*, version 5.618, Bruker Analytical X-ray System, **2000**.
- [43] *SAINT-NT*, Version 6.04, Bruker Analytical X-ray System, **2001**.
- [44] *SHELXTL-NT*, Version 6.10, Bruker Analytical X-ray System, **2000**.
- [45] L. J. Farrugia, *WinGX*, Version 1.64, *An Integrated System of Windows Programs for the Solution, Refinement and Analysis of Single-Crystal X-ray Diffraction Data*, Department of Chemistry, University of Glasgow, **2003**.

Received: June 14, 2010

Published Online: October 5, 2010